Research in Astronomy and Astrophysics, 24:025017 (6pp), 2024 February https://doi.org/10.1088/1674-4527/ad1d2a

GRB 200612A: An Ultralong Gamma-Ray Burst Powered by Magnetar Spinning Down

Liang-Jun Chen (陈良军), Xiang-Gao Wang (王祥高), De-Long Yang (杨德龙), and En-Wei Liang (梁恩维)
Guangxi Key Laboratory for Relativistic Astrophysics, School of Physical Science and Technology, Guangxi University, Nanning 530004, China; wangxg@gxu.edu.cn, lew@gxu.edu.cn
Received 2023 August 2; revised 2023 December 19; accepted 2023 December 29; published 2024 February 7

Abstract

GRB 200612A could be classified as an ultralong gamma-ray burst due to its prompt emission lasting up to ∼1020 s and the true timescale of the central engine activity $t_{\rm burst} \geqslant 4 \times 10^4$ s. The late X-ray light curve with a decay index of $\alpha = 7.53$ is steeper than the steepest possible decay from an external shock model. We propose that this X-ray afterglow can be driven by dipolar radiation from the magnetar spindown during its early stage, while the magnetar collapsed into the black hole before its spindown, resulting in a very steep decay of the late X-ray light curve. The optical data show that the light curve is still rising after 1.1 ks, suggesting a late onset. We show that GRB 200612A's optical afterglow light curve is fitted with the forward shock model by Gaussian structured off-axis jet. This is a special case among GRBs, as it may be an ultralong gamma-ray burst powered by a magnetar in an off-axis observation scenario.

Key words: (stars:) gamma-ray burst: individual (GRB 200612A) – (stars:) gamma-ray burst: general – stars: magnetars

1. Introduction

As the most energetic events in astronomy, gamma-ray bursts (GRBs) have been extensively studied. The GRBs whose prompt emission duration is less than 2 s are classified as short-GRBs, while those lasting for more than 2 s are called long-GRBs. In the histogram of duration, short GRBs peak at 0.2–0.3 s, while long GRBs peak at 20–30 s (Kouveliotou et al. 1993) and ranging from ∼2 s up to several hundred seconds in the observer frame.

Some GRBs have been reported with an extraordinary duration of 10^4 s, known as ultralong GRBs. It has been debated whether these belong to a new distinct class of events or if they are similar to long GRBs. The former hypothesis suggests that the progenitors of these ultralong GRBs may be blue supergiants (Gendre et al. 2013; Nakauchi et al. 2013; Levan et al. 2014; Huang et al. 2020), while the latter hypothesis proposes that ultralong GRBs share the same progenitors with long gamma-ray bursts, representing the tail of the distribution of long GRBs (Virgili et al. 2013; Evans et al. 2014). Zhang et al. (2014) proposed defining ultralong GRBs based on the true timescale of the central engine activity ($t_{\rm burst}$). The $t_{\rm burst}$ distribution of their "good" sample shows an apparent bimodal distribution with a narrow, significant peak at ∼355 s, and a wider, less significant peak at $\sim 2.8 \times 10^4$ s, respectively. Gao et al. (2017) obtained similar results as a narrow, significant peak at 173.8 s and a wider, less significant peak at $\sim 2.75 \times 10^4$ s , respectively. As an example of an ultralong case, GRB 101225 shows that plateau and extremely sharp flux drop could present in X-ray afterglow, it may be driven by a newborn magnetar (Lü et al. 2018; Zou et al. 2019). Both the normal long GRB model and the blue supergiant model will launch an ultra-relativistic jet. Usually, we assume that observations are occurring on-axis, but some off-axis GRBs have been observed, such as GRB 170817A (Abbott et al. 2017). An observer at $\theta_v < \theta_j$, where θ_v is the viewing angle, θ_j is the jet half-opening angle, should see a light curve very similar to that for an on-axis observer, an observer at $\theta_v > \theta_j$ will see a rising light curve at early times, peaking when the jet Lorentz factor is $\sim 1/\theta_v$, and approaching that is seen by an on-axis observer at later times (Woods & Loeb 1999; Granot et al. 2002).

GRB 200612A is a special case that may be an ultralong gamma-ray burst driven by a magnetar spinning down in an off-axis scenario. The structure of the paper is as follows. The observations are presented in Section 2. In Section 3, we perform the analyses of afterglow. Then, in Section 4, we model the light curves. Our conclusions and discussion are given in Section 5.

2. Observations

GRB 200612A triggered the Swift Burst Alert Telescope (BAT) on 2020 June 12 at 04:39:37 UT (denoted as T_0 in this paper). The mask-weighted light curve shows a complex structure that starts at $\sim T_0 - 20$ s and lasts until $\sim T_0 + 200$ s. T_{90} (15–350 keV) estimated by BAT is $T_{90,\rm BAT} = 171.48 \pm 19.74$ s (Markwardt et al. 2020; Sonbas

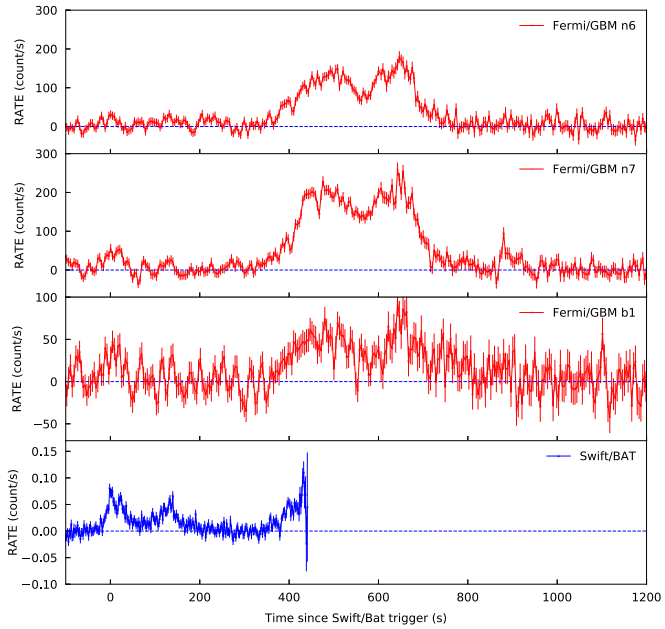

Figure 1. The prompt emission light curves of GRB 200612A with 4.096 s binning. Observations from the Fermi/GBM detectors and Swift/BAT detectors are represented by red solid and blue solid lines, respectively.

et al. 2020). At 04:49:38.68 UT ($T_0 + 10$ minutes), the Fermi Gamma-Ray Burst Monitor (GBM) triggered and located GRB 200612A. Fermi GBM Team report they detected this burst and provide $T_{90,\mathrm{GBM}} \sim 88$ s (50–300 keV) at GCN circular. In Fermi GBM Burst Catalog,[1] they provide $T_{90,\mathrm{GBM}} = 984 \pm 65$ s. The light curve of Fermi/GBM and Swift/BAT is presented in Figure 1. GRB 200612A was also detected by Konus–Wind (Svinkin et al. 2020). They observed that the burst light curve shows four emission episodes in the interval from $\sim T_0$ to $\sim T_0 + 1020$ s. They classified this burst as an ultralong GRB. As observed by Konus–Wind, the burst had a fluence of $4.08^{+1.04}_{-0.34} \times 10^{-5}$ erg cm^{-2}.

The Swift X-Ray Telescope (XRT) began observing the field at 04:41:04.7 UT ($T_0 + 87.7$ s). The enhanced Swift/XRT position is R.A., decl. (J2000) $= 20^{\mathrm{h}}10^{\mathrm{m}}48\overset{\mathrm{s}}{.}49$, $-45°20'07\overset{''}{.}8$ with an uncertainty of $1\overset{''}{.}5$. The Swift Ultraviolet/Optical Telescope (UVOT) took a finding chart exposure of 150 s with the white filter starting at $T_0 + 95$ s. However, no credible afterglow candidate has been found in their initial data products.

MASTER-OAFA robotic telescope located in Argentina (OAFA observatory of San Juan National University) was pointed to GRB200612A at 2020 June 12 04:47:52 UT ($T_0 + 495$ s). They found an optical transient within Swift error-box (R.A. $= 302.679$, decl. $= -45.3569$, $r = 0.05$) with

[1] https://heasarc.gsfc.nasa.gov/cgi-bin/W3Browse/w3hdprods.pl?files=P&Target=heasarc%Ffermigbrst%7C%7C%7C%5F%5Frow=586%7C%7C&Coordinates=Equatorial&Equinox=2000

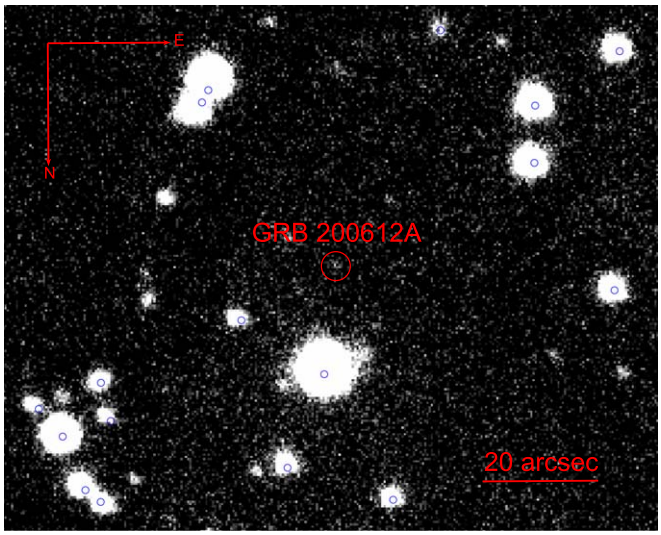

Figure 2. The *R*–band image of GRB 200612A taken on 2020 June 14, with four frames combined. Echo frame exposure 300 s was taken from 00:45:34 to 01:01:58 UTC, i.e., 1.84 days after the trigger of the GRB.

17.9 Mag at $T_0 + 1050$ s (Lipunov et al. 2020) and 17.5 Mag at $T_0 + 1172$ s (Tiurina 2020). The 60 cm BOOTES-3/YA robotic telescope at NIWA Lauder in Otago (New Zealand) began observing the position reported by Swift/XRT at 09:51:32 UT($\sim$5.2 hr after trigger). In the co-added image (20 exposures of 60 s each in the clear filter), no source is found at the position, and the upper limit is 20.3 mag (Hu et al. 2020).

We observed the field of GRB 200612A with the LCO 1 m Sinistro instrument starting at 2020 June 14 00:45:34 UT ($T_0 + 1.84$ days), four images in the *R*–band were obtained (exposures 300 s each). A weak source was found within the Swift error box. Figure 2 shows the *R*–band image of the field of GRB 200612A taken at $T_0 + 1.84$ days. The data reduction was carried out following the standard routine in the IRAF package (Tody 1986). The photometric result is $R = 22.90 \pm 0.35$, not corrected for the Galactic extinction.

3. Data Analysis

We fit the X-ray light curve with a single power-law function

$$F = F_0 t^{-\alpha}, \tag{1}$$

and a broken power-law function

$$F = F_1 \left[\left(\frac{t}{t_b} \right)^{\omega\alpha_1} + \left(\frac{t}{t_b} \right)^{\omega\alpha_2} \right]^{-1/\omega}, \tag{2}$$

where F_1 is the flux at the break time (t_b), α_1 and α_2 are the afterglow flux decay indices before and after t_b, respectively, and ω is a smoothness parameter which represents the sharpness of break. Five phases comprise this X-ray light curve (Figure 3). Phases I and II form a flare with $\alpha_1 = -1.56^{+0.16}_{-0.17}$,

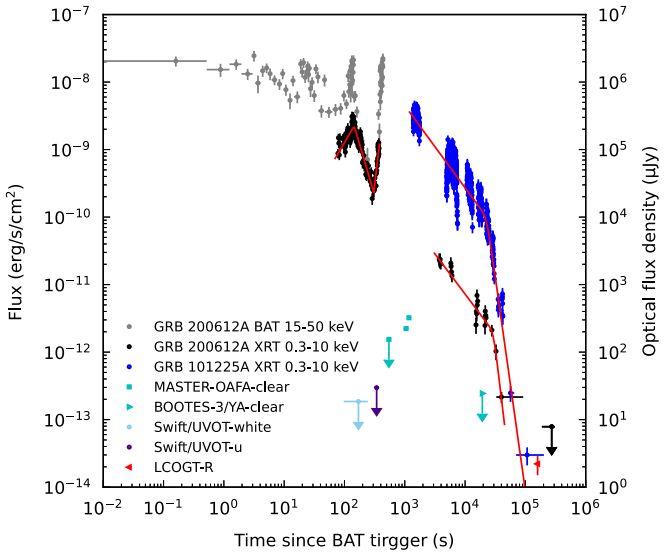

Figure 3. Broadband light curve of GRB 200612A, including γ-ray and X-ray flux and optical flux densities. The red solid line represents the best-fitting result for the X-ray afterglow using a power-law or broken power-law model. The blue point is the X-ray afterglow of GRB 101225A.

$\alpha_2 = 3.06^{+0.10}_{-0.10}$ and peak at $t_p = 145^{+3}_{-4}$ s, Phase III rises from ~300 s, then Swift satellite suffers from Earth occultation, so there are no data between 380 and 3700 s. Phases IV and V are fit to broken power-law function with $\alpha_4 = 1.18^{+0.07}_{-0.08}$, $\alpha_5 = 7.53^{+0.93}_{-1.11}$ and a break time at $t_b = 3.09^{+0.27}_{-0.14} \times 10^4$ s. The steep decay in Phase V is inconsistent with an external shock model. The steepest possible decay from an external shock occurs after a jet break. The post-jet-break decay slope can be as steep as p, where p is the electron spectral index (Rhoads 1999; Sari et al. 1999). Afterglow modeling suggests that p is typically between 1.5 and 3; however, $\alpha_5 = 7.53^{+0.93}_{-1.11}$ obviously deviates from this range. According to the definition of $t_{\rm burst}$ proposed by Zhang et al. (2014) and Gao et al. (2017), we obtained $t_{\rm burst} \geqslant 4.01 \times 10^4$ s of this GRB, aligning with the definition of ultralong GRBs.

4. Model and Result

The X-ray light curve of GRB 200612A breaks to a steep decay at t_b, which is far too steep for a jet break. A rapid drop of the X-ray flux with a decay index steeper than –3 followed by the plateau in some cases which is considered as evidence of a magnetar collapsing into a black hole (Troja et al. 2007). We propose that a newborn magnetar powered this X-ray emission, and it collapsed to form a black hole at t_b, resulting in the decay of Phase V is extremely steep. The newborn magnetar spindown by losing its rotational energy through two channels (electromagnetic dipolar radiation and gravitational wave radiation Shapiro & Teukolsky 1983), the electromagnetic emission luminosity would evolve with time as $L \propto (1 + t/\tau)^{-\alpha}$, where $\alpha = 1$ when gravitational-wave emission dominates the spindown losses, and $\alpha = 2$ when electromagnetic losses dominant instead (Dai & Lu 1998; Zhang & Mészáros 2001). Usually, the stage where gravitational-wave emission dominates the spindown energy lost should end in early time. There is more likely electromagnetic dipolar radiation dominating before the light curve breaks at t_b. Therefore we describe this X-ray light curve as follows:

$$L(t) = \begin{cases} L_{\rm MD}\left(1 + \dfrac{t}{\tau(1+z)}\right)^{-2}, & t < t_b \\ L_{\rm MD}\left(1 + \dfrac{t_b}{\tau(1+z)}\right)^{-2}\left(\dfrac{t}{t_b}\right)^{-\alpha}, & t > t_b \end{cases}, \quad (3)$$

where $L_{\rm MD}$ is the characteristic spindown luminosity, and τ is the characteristic spindown timescale. Since this burst lacks a measured redshift, we assumed its redshift to be $z = 2.27$, based on the average redshift obtained from the long GRB sample (Campisi et al. 2010).

There is sparse data in the optical band; however, we can still infer that the onset is later than 1.1 ks. The onset time distribution ranges in the GRBs population from 30 to 3000 s (Liang et al. 2013). The off-axis jet model may explain the observed later onset afterglow (Granot et al. 2002; Sato et al. 2021). The jet with a large Lorentz factor has a strong relativistic beaming effect, making the afterglow emission very dim for the off-axis observer. As the jet decelerates, the beaming effect weakens, leading to a rising in afterglow light curves. We attribute GRB 200612A optical emissions to be produced by external forward shock in an axisymmetric Gaussian structured off-axis jet case. The external forward shock model (Sari et al. 1998; Huang et al. 1999) requires a few parameters to calculate the afterglow in multiband. These parameters include the isotropic-equivalent kinetic energy $E_{K,\rm iso}$, the initial bulk Lorentz factor Γ_0, the ambient interstellar matter (ISM) which is assumed to be uniform with the number density n_0, the fractions of shock energy that go to electrons and magnetic fields (ϵ_e and ϵ_B), the electron spectral index p, the jet opening half-angle θ_j and viewing angles θ_v. We consider the Gaussian structured jet as:

$$E_{K,\rm iso}(\theta) = E_{K,\rm iso,0} \exp\left(-\frac{\theta^2}{2\theta_c^2}\right), \quad (4)$$

$$M_{\rm iso}(\theta) = M_{\rm iso,0} \exp\left(-\frac{\theta^2}{2\theta_c^2}\right), \quad (5)$$

where $E_{K,\rm iso}(\theta)$ and $M_{\rm iso}(\theta)$ represent the isotropic-equivalent kinetic energy and isotropic-equivalent masses of the jet at θ, respectively. The initial Lorentz factor at θ is set as $\Gamma_0(\theta) = E_{K,\rm iso}(\theta)/M_{\rm iso}(\theta)c^2 + 1$. θ is the polar angle with respect to the jet axis, θ_c is characteristic angle for the jet. $E_{K,\rm iso}(\theta)$ and $M_{\rm iso}(\theta)$ are zero when θ is greater than the

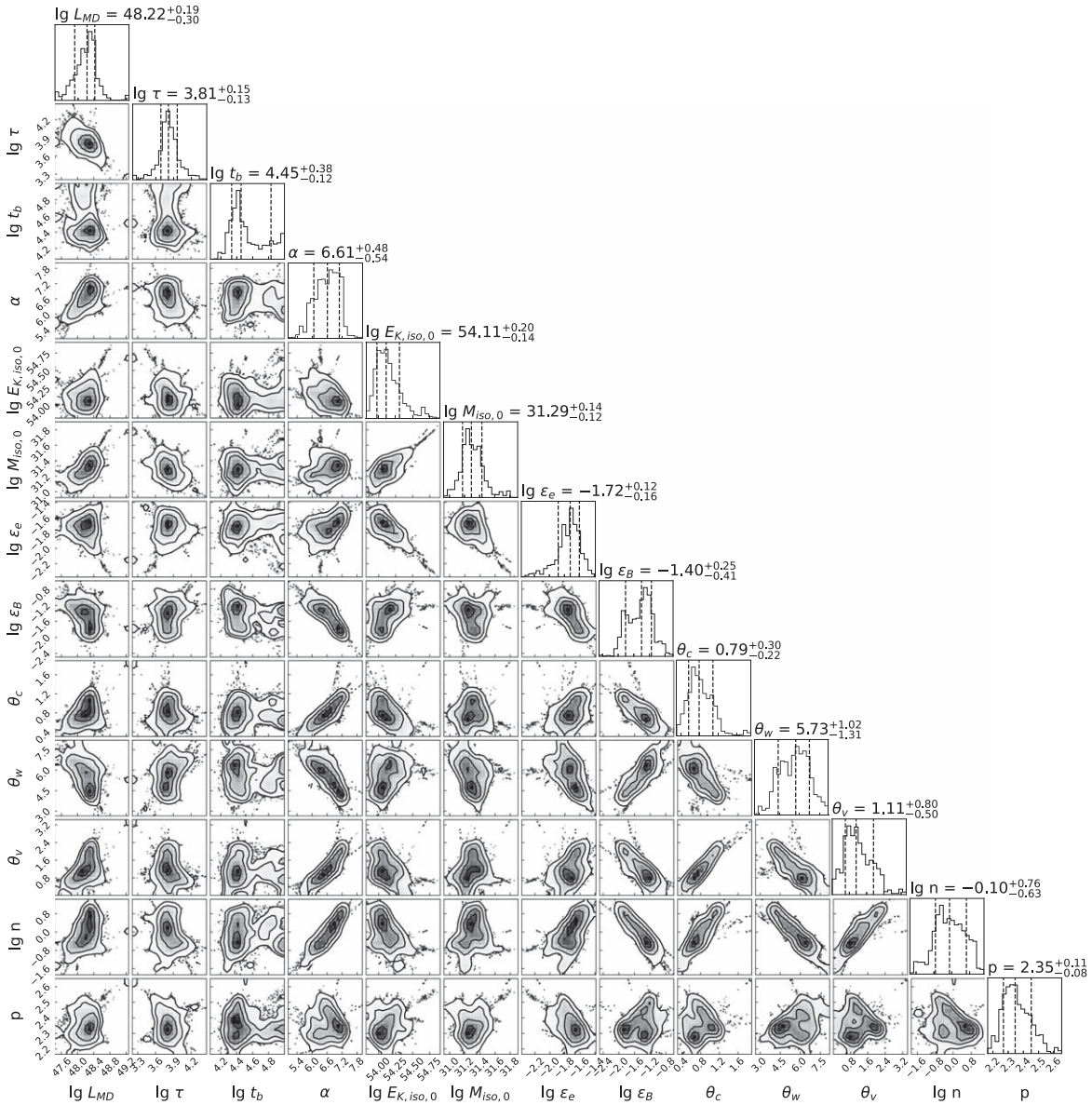

Figure 4. The posterior distributions of parameters for the best-fit light curves of GRB 200612A.

truncation angle θ_w. We performed a Markov Chain Monte Carlo exploration of the multidimensional parameter space using emcee (Foreman-Mackey et al. 2013). The one- and two-dimensional marginalized views of the posterior distribution for the Gaussian jet model fits show in Figure 4. The parameter estimation priors and marginalized posteriors are reported in Table 1, the optimal fitting results are shown in Figure 5. Both X-ray and optical data comply with the model lines.

5. Conclusions and Discussion

GRB 200612A prompt emission lasting ∼1020 s and the true timescale of the central engine activity $t_{\rm burst} \geqslant 4 \times 10^4$ s, could be classified into an ultralong gamma-ray burst. The X-ray light curve drops rapidly with a decay index of ~ -7 post break time $t_b \sim 3 \times 10^4$ s. This is the signal of a center engine turns off. The newly born magnetar dipolar radiation could power this X-ray before t_b, then collapsing into a black hole, making the light curve decay sharply.

This burst's redshift has not been directly measured. We assume its redshift to be $z = 2.27$. We estimated the characteristic spindown luminosity to be $L_{\rm MD} \sim 1.7 \times 10^{48}$ erg s^{-1}, while the characteristic spindown timescale is estimated to be $\tau \sim 6.4 \times 10^3$ s. The collapse into a black hole is projected to occur at $t_b \sim 2.8 \times 10^4$ s. With the fluence of

Table 1
Parameter Estimation Priors and Marginalized Posteriors for the Afterglow of GRB 200612A

Parameter	Unit	Prior Form	Bounds	Posterior
$\log_{10} L_{\rm MD}$	erg s^{-1}	uniform	[30, 60]	$48.22^{+0.19}_{-0.30}$
$\log_{10} \tau$	s	uniform	[3, 5]	$3.81^{+0.15}_{-0.13}$
$\log_{10} t_b$	s	uniform	[3, 5]	$4.45^{+0.38}_{-0.12}$
α	...	uniform	[1, 10]	$6.61^{+0.48}_{-0.54}$
$\log_{10} E_{K,iso,0}$	erg	uniform	[47, 59]	$54.11^{+0.20}_{-0.14}$
$\log_{10} M_{iso,0}$	g	uniform	[25, 35]	$31.29^{+0.14}_{-0.12}$
$\log_{10} \epsilon_e$	...	uniform	[−8, 0]	$-1.72^{+0.12}_{-0.16}$
$\log_{10} \epsilon_B$	...	uniform	[−8, 0]	$-1.40^{+0.25}_{-0.41}$
θ_c	degree	uniform	[0.1, 30]	$0.79^{+0.30}_{-0.22}$
θ_w	degree	uniform	[0.1, 60]	$5.73^{+1.02}_{-1.31}$
θ_v	degree	uniform	[0, 30]	$1.11^{+0.80}_{-0.50}$
$\log_{10} n$	cm^{-3}	uniform	[−5, 5]	$1.11^{+0.76}_{-0.63}$
p	...	uniform	[2, 3]	$2.35^{+0.11}_{-0.08}$

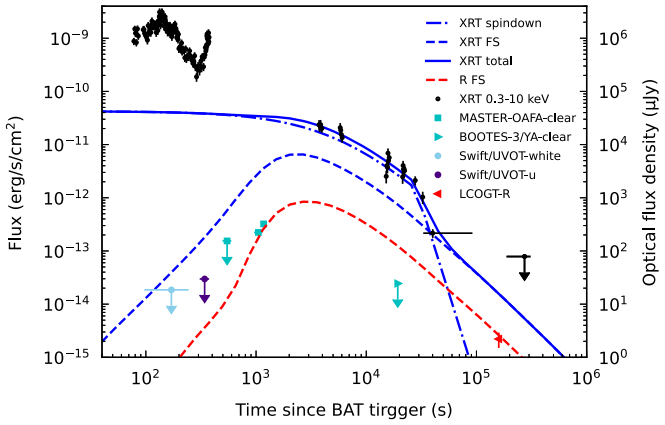

Figure 5. Modeling the optical and X-ray light curves with magnetar spindown adds external forward shock model in off-axis case. The dashed–dotted and dashed lines in blue are dipole radiation of magnetar spindown and off-axis external forward shock model at X-ray (0.3–10 keV), respectively, the blue solid line is the total flux calculated from our model. The red solid line is flux density calculated from the off-axis external forward shock model.

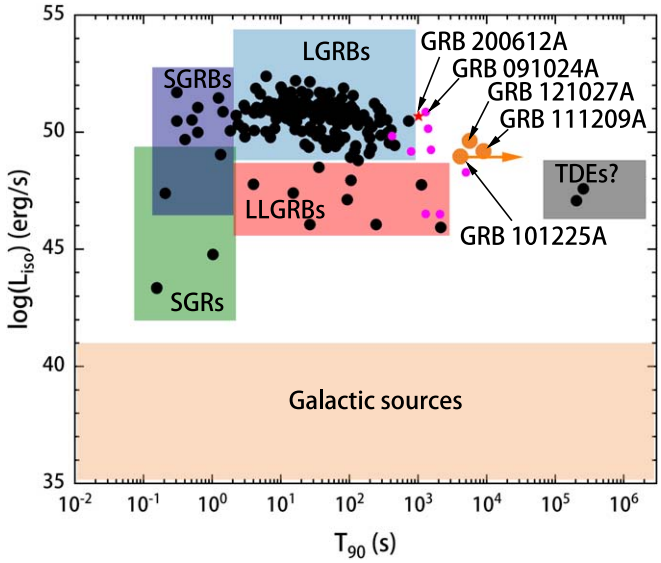

Figure 6. The isotropic luminosity vs. the duration time of different classes of transients. The red star is GRB 200612A with assumed redshift $z = 2.27$. The magenta dots are ultralong GRBs taken from Huang et al. (2020), they collect these from (Nicastro et al. 2004; Campana et al. 2006; Starling et al. 2011; Zhang et al. 2012; Virgili et al. 2013; Zauderer et al. 2013; Evans et al. 2014; Cucchiara et al. 2015; Frederiks et al. 2016; Hou et al. 2018), the orange dots are ultralong GRBs taken from Levan et al. (2014), and other transient data are taken from Levan et al. (2014).

$4.08^{+1.04}_{-0.34} \times 10^{-5}$ erg cm^{-2} (Svinkin et al. 2020), the isotropic-equivalent luminosity will be $L_{\gamma,\rm iso} = 4.8^{+1.2}_{-0.4} \times 10^{50}$ erg s^{-1}. The isotropic X-ray energy released during the magnetic dipole radiation epoch is $E_{\rm X,iso} = L_{\rm MD} t_b/(1+z) = 1.4^{+3.9}_{-0.9} \times 10^{52}$ erg. One can define the radiative efficiency for a magnetar to convert its spindown energy to radiation as $\eta_{\rm X} = E_{\rm X,iso}/(E_{\rm X,iso} + E_{K,\rm iso})$, then obtain $\eta_{\rm X} = 0.011^{+0.039}_{-0.007}$. Furthermore, we estimate the strength of the dipolar magnetic field as $B_{p,15} = 2.05(I_{45} R_6^{-3} L_{\rm MD,49}^{-1/2} \tau_3^{-1})$ G and the initial spin period as $P_{0,-3} = 1.42(I_{45}^{1/2} L_{\rm MD,49}^{-1/2} \tau_3^{-1/2})$ s, where Q_n is $Q/10^n$ in the cgs units. Taking the moment of inertia $I = 10^{45}$ g cm^2, and $R = 10^6$ cm, we derive $B_p = 0.78^{+0.71}_{-0.34} \times 10^{15}$ G and $P_0 = 1.37^{+0.88}_{-0.45}$ ms. These values are in good agreement with those reported by Lü & Zhang (2014).

The optical data show that the light curve still rising post ∼1.1 ks, has a late onset, this is in accord with the character of the off-axis observer case. We model the optical afterglow using an off-axis Gaussian structured jet model and find that the viewing angle is $\theta_v \sim 1.^\circ 1$. The truncation angle $\theta_w \sim 5.^\circ 7$ is great than θ_v, allowing the prompt emission to be observed.

As shown in Figure 6, although the duration T_{90} of GRB 200612A is much smaller than several famous ultralong GRBs, for instance GRB 101225A ($T_{90} > 7000$ s; Levan et al. 2014), GRB 111209 ($T_{90} \sim 10000$ s; Golenetskii et al. 2011), GRB 121027A ($T_{90} \sim 6000$ s; Levan et al. 2014), but it still located in same zone of the ultralong GRBs reported at (Huang et al. 2020), e.g., the magenta dots in Figure 6, and nearby the ultralong GRB 091024A ($T_{90} = 1300$ s, Virgili et al. 2013). GRB 101225A is a famous ultralong GRB with $T_{90} > 7000$ s and $t_{\rm burst} \geqslant 1.07 \times 10^5$ s (Campana et al. 2011; Thöne et al. 2011; Nakauchi et al. 2013; Levan et al. 2014; Zhang et al. 2014; Gao et al. 2017). Its X-ray exhibits a normal power-law decay segment ($F \propto t^{-1.21\pm0.02}$) followed by an extremely sharp flux drop ($F \propto t^{-6.35\pm0.34}$). The possible origin of ultralong GRB 101225A may be consistent with the magnetar spin-down emission dominated and collapses to a black hole at a later time (Lü et al. 2018; Zou et al. 2019). The decay index is consistent with Phase IV ($\alpha_4 = 1.18^{+0.07}_{-0.08}$) and V

($\alpha_5 = 7.53^{+0.93}_{-1.11}$) of GRB 200612A with the error. The similarity of the light curves suggests that GRB 200612A and GRB 101225A may have the same origin.

Classifying GRBs by duration is rough. Virgili et al. (2013) take the critical duration as 1000 s, while Levan et al. (2014) suggest that an ultralong burst high-energy emission should be lasting to $\sim 10^4$ s. However, the origin of ultralong bursts remains a subject of debate. Tidal disruption events (Shcherbakov et al. 2013; MacLeod et al. 2014) and a GRB with a blue supergiant progenitor (Nakauchi et al. 2013) are potential explanations for these ultralong bursts. However, Virgili et al. (2013) propose that ultralong GRBs may represent the tail of the duration distribution of the long GRB population. In this study, we do not attempt to ascertain the progenitor of GRB 200612A. We utilize dipolar radiation from magnetar and external shock radiation from an off-axis jet to model the afterglow light curve of this burst.

Acknowledgments

This work is supported by the National Natural Science Foundation of China (Nos. U1938201 and 12373042).

ORCID iDs

Liang-Jun Chen
(陈良军) https://orcid.org/0009-0007-7188-3196

References

Abbott, B. P., Abbott, R., Abbott, T. D., et al. 2017, ApJL, 848, L13
Campana, S., Lodato, G., D'Avanzo, P., et al. 2011, Natur, 480, 69
Campana, S., Mangano, V., Blustin, A. J., et al. 2006, Natur, 442, 1008
Campisi, M. A., Li, L. X., & Jakobsson, P. 2010, MNRAS, 407, 1972
Cucchiara, A., Veres, P., Corsi, A., et al. 2015, ApJ, 812, 122
Dai, Z. G., & Lu, T. 1998, A&A, 333, L87
Evans, P. A., Willingale, R., Osborne, J. P., et al. 2014, MNRAS, 444, 250
Foreman-Mackey, D., Hogg, D. W., Lang, D., & Goodman, J. 2013, PASP, 125, 306
Frederiks, D., Golenetskii, S., Aptekar, R., et al. 2016, GCN, 20141, 1
Gao, H., Ren, A.-B., Lei, W.-H., et al. 2017, ApJ, 845, 51
Gendre, B., Stratta, G., Atteia, J. L., et al. 2013, ApJ, 766, 30
Golenetskii, S., Aptekar, R., Mazets, E., et al. 2011, GCN, 12663, 1
Granot, J., Panaitescu, A., Kumar, P., & Woosley, S. E. 2002, ApJL, 570, L61
Hou, S.-J., Liu, T., Xu, R.-X., et al. 2018, ApJ, 854, 104
Hu, Y. D., Fernandez-Garcia, E., Castro-Tirado, A. J., et al. 2020, GCN, 27919, 1
Huang, Y., Luo, Q., Zhang, B., & Xiong, S. 2020, SSPMA, 50, 129504
Huang, Y. F., Dai, Z. G., & Lu, T. 1999, MNRAS, 309, 513
Kouveliotou, C., Meegan, C. A., Fishman, G. J., et al. 1993, ApJL, 413, L101
Levan, A. J., Tanvir, N. R., Starling, R. L. C., et al. 2014, ApJ, 781, 13
Liang, E.-W., Li, L., Gao, H., et al. 2013, ApJ, 774, 13
Lipunov, V., Gorbovskoy, E., Kornilov, V., et al. 2020, GCN, 27917, 1
Lü, H.-J., & Zhang, B. 2014, ApJ, 785, 74
Lü, H.-J., Zou, L., Lan, L., & Liang, E.-W. 2018, MNRAS, 480, 4402
MacLeod, M., Goldstein, J., Ramirez-Ruiz, E., Guillochon, J., & Samsing, J. 2014, ApJ, 794, 9
Markwardt, C. B., Barthelmy, S. D., Cummings, J. R., et al. 2020, GCN, 27924, 1
Nakauchi, D., Kashiyama, K., Suwa, Y., & Nakamura, T. 2013, ApJ, 778, 67
Nicastro, L., in't Zand, J. J. M., Amati, L., et al. 2004, A&A, 427, 445
Rhoads, J. E. 1999, ApJ, 525, 737
Sari, R., Piran, T., & Halpern, J. P. 1999, ApJL, 519, L17
Sari, R., Piran, T., & Narayan, R. 1998, ApJL, 497, L17
Sato, Y., Obayashi, K., Yamazaki, R., Murase, K., & Ohira, Y. 2021, MNRAS, 504, 5647
Shapiro, S. L., & Teukolsky, S. A. 1983, Black Holes, White Dwarfs, and Neutron Stars: The Physics of Compact Objects (New York: Wiley)
Shcherbakov, R. V., Pe'er, A., Reynolds, C. S., et al. 2013, ApJ, 769, 85
Sonbas, E., Gronwall, C., Klingler, N. J., et al. 2020, GCN, 27915, 1
Starling, R. L. C., Wiersema, K., Levan, A. J., et al. 2011, MNRAS, 411, 2792
Svinkin, D., Golenetskii, S., Aptekar, R., et al. 2020, GCN, 27922, 1
Thöne, C. C., de Ugarte Postigo, A., Fryer, C. L., et al. 2011, Natur, 480, 72
Tiurina, N. 2020, GCN, 27920, 1
Tody, D. 1986, Proc. SPIE, 627, 733
Troja, E., Cusumano, G., O'Brien, P. T., et al. 2007, ApJ, 665, 599
Virgili, F. J., Mundell, C. G., Pal'shin, V., et al. 2013, ApJ, 778, 54
Woods, E., & Loeb, A. 1999, ApJ, 523, 187
Zauderer, B. A., Berger, E., Margutti, R., et al. 2013, ApJ, 767, 161
Zhang, B., & Mészáros, P. 2001, ApJL, 552, L35
Zhang, B.-B., Burrows, D. N., Zhang, B., et al. 2012, ApJ, 748, 132
Zhang, B.-B., Zhang, B., Murase, K., Connaughton, V., & Briggs, M. S. 2014, ApJ, 787, 66
Zou, L., Zhou, Z.-M., Xie, L., et al. 2019, ApJ, 877, 153